ASTRONOMY
AND
ASTROPHYSICS

Physical properties of the pulsating hydrogen-deficient star LSS 3184 (BX Cir) *

V. M. Woolf and C. S. Jeffery

Armagh Observatory, College Hill, Armagh, BT61 9DG, Northern Ireland
email: vmw@star.arm.ac.uk, csj@star.arm.ac.uk

Abstract. We report new determinations of the radius and mass of the pulsating helium-rich, hydrogen-deficient star LSS 3184 (BX Cir) using measurements of radial velocity and angular radius throughout its pulsation cycle. Measurements of radial velocity, and thus changes in stellar radius ($\Delta R_\star$), were made using Anglo-Australian Telescope echelle spectra. *Hubble Space Telescope* ultraviolet spectra and ground-based BV photometry were used to find temperatures and fluxes throughout the pulsation cycle. The temperatures and fluxes were used to find the angular radius of the star (α). The α, $\Delta\alpha$, and ΔR values thus found were used to calculate the mean stellar radius $\langle R_\star \rangle = 2.31 \pm 0.10 R_\odot$. If we use the previously determined $\log g = 3.35 \pm 0.1$ for LSS 3184 and our radius estimate, we find its mass to be $M_\star = 0.42 \pm 0.12 M_\odot$.

Key words: stars: chemically peculiar – stars: oscillations – stars: variables – stars: individual: LSS 3184

1. Introduction

Pulsations in stars provide tools for researchers in several fields of astronomy. They provide standard candles for measuring Galactic and extragalactic distances and they provide methods for measuring stellar parameters, even below the directly observable photosphere. Pulsations in hydrogen-deficient, helium-rich stars such as extreme helium, R Coronae Borealis, and hydrogen-deficient carbon stars have not been studied in as much detail as those in stars with more 'normal' chemical abundances. While this is partly understandable since most pulsating stars have normal compositions, studying stars with little or no hydrogen is important to allow tests of pulsation theory.

Extreme helium stars, as their name would imply, have weak or non-existent hydrogen absorption lines and very large helium abundances ($\gtrsim$ 99 per cent). Two extreme helium stars, V652 Her and LSS 3184, are known to pulsate. Saio (1993) showed that in extreme helium stars with temperatures around 2×10^5 K, like V652 Her, the κ-mechanism caused by iron-group (Z-bump) opacity can excite the observed pulsations. Saio (1994, 1995) predicted that LSS 3184 should pulsate because of its location in the Z-bump instability finger. Kilkenny & Koen (1995) discovered that LSS 3184 shows photometric variations with a period of about 0.107 d. The similarity of V652 Her and LSS 3184 in temperature, surface gravity, and pulsation period implies that they are very similar in other physical parameters.

Kilkenny et al. (1999) have recently reported an observational analysis of LSS 3184, including a determination of its photometric period (0.1066 d). In addition, they used medium resolution ($\lambda/\Delta\lambda \approx 4000$) spectra to measure radial velocity variations and to show that the photometric variability is caused by pulsations. Drilling, Jeffery, & Heber (1998) reported an analysis of LSS 3184 in which they found $T_{\rm eff} = 23\,300 \pm 700$ K, $\log g = 3.35 \pm 0.1$ and $n_{\rm H}/n_{\rm He} \leq 0.00015$. Kilkenny et al. (1999) report that using the radius they determined and $\log g$ from Drilling et al. (1998) gives a mass of $0.15 M_\odot$, which is much smaller than $0.7 M_\odot$, the mass accepted for V652 Her (Lynas-Gray et al. 1984), and small enough to imply that some input parameter or procedure is in error.

In this paper we report an analysis of LSS 3184 using high resolution optical spectra for radial velocity measurement and ultraviolet *Hubble Space Telescope* (*HST*) spectra and ground-based BV photometry for temperature, luminosity, and angular radius measurement. The new data provide better temperature and angular radius estimates and a much cleaner radial velocity curve for the star, allowing a more reliable estimate of its radius and mass than was possible previously.

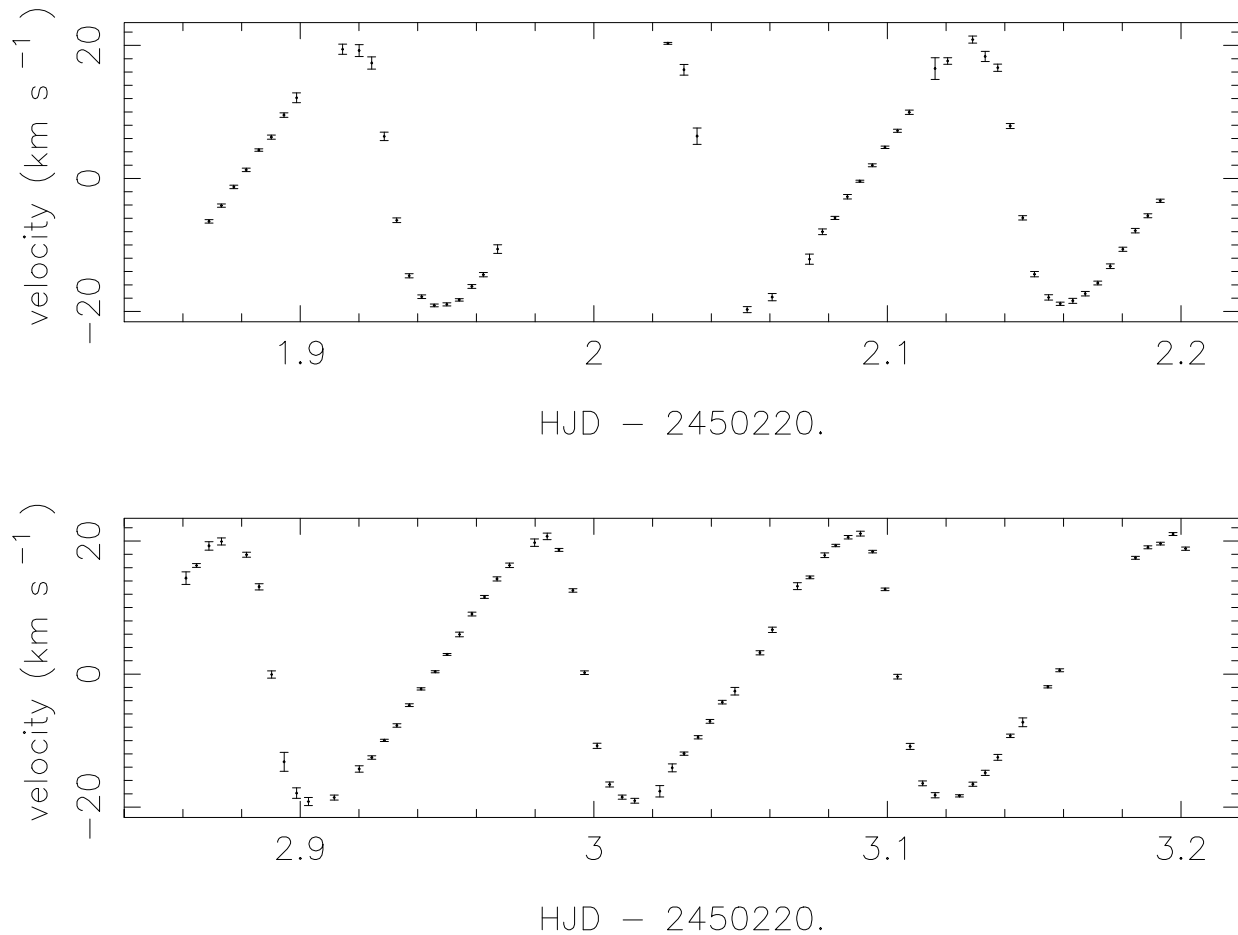## 2. Observations and data reduction

Fig. 1. Plot showing velocity and phase coverage for LSS 3184 spectroscopic observations, with error bars shown for velocity. Note that the velocity here is not corrected for projection effects.

2.1. AAT visible spectral observations

Spectra of LSS 3184 were obtained during the nights of 1996 May 18 and 19 using the University College London Echelle Spectrograph at the 3.9-m Anglo-Australian Telescope. Exposure times were between 4 and 5 minutes. Standard IRAF packages were used for bias and flat field correction, reducing echelle orders to one dimensional spectra, and applying the wavelength scale using thorium-argon spectra. As the wavelengths covered by adjacent orders overlapped, the spectra covered the range 3850–5055 Å completely. The spectral resolution was $\lambda/\Delta\lambda \approx 48\,000$. Velocity corrections for Earth's motion were found for each exposure using RVCORRECT and were applied using DOPCOR.

2.2. Hubble Space Telescope ultraviolet observations

Ultraviolet spectra of LSS 3184 were obtained using the Faint Object Spectrograph of the *HST*. Observations were made in RAPID mode using the blue detector, the 0″.86 square aperture and grating G160L over three orbits on 1997 February 7. Data files reduced using the most recent

calibration files were downloaded from the *HST* archives on 1999 October 12. Individual exposures were made approximately 19.25 seconds apart. The usable part of the spectra covered the range 1150–2500 Å. Based on the ephemeris of Kilkenny et al. (1999), observations during the three orbits covered the phase (ϕ) ranges from 0.3154–0.6099, 0.9327–0.2376, and 0.5602–0.8651, where maximum V magnitude is at $\phi = 0$ and again at $\phi = 1$. Thus the star was observed by the *HST* over 85.5 per cent of its pulsational cycle.

3. Analysis

3.1. Radial velocity determinations

The velocity shifts between spectra were measured using the cross correlation package FXCOR in IRAF. For each measurement the velocities found from 28 of the 35 orders of the echelle spectra were used to find a weighted average velocity. Weights for the averaging were the inverse of the velocity errors reported by FXCOR. The unused spectral orders either had no strong absorption lines or had strong

interstellar lines which did not allow a reliable stellar velocity determination.

The procedure took two iterations. In the first iteration the best results were obtained by using the sum of all the second night's LSS 3184 spectra as the cross correlation template for the first night's spectra and vice versa. The spectra from both nights were then shifted by the velocities thus found and co-added to provide the template for the second iteration. The absorption lines in the second template were much sharper, as the velocity smearing due to the stellar pulsations was effectively removed. A third iteration was performed with the spectra shifted by the velocities found in the second iteration before co-adding to make the template, but the velocities from the third iteration were effectively identical to those from the second. The velocities from the second iteration, shifted so that the mean velocity is zero, are shown in Fig. 1. Error bars show the weighted standard deviations of the velocity from the echelle orders. Gaps are present in the data where clouds prevented observations. From the the data in Fig. 1, we find that the peak-to-peak radial velocity variation is 40.0 ± 0.3 km s^{-1}, which is larger than 30 km s^{-1}, the value found by Kilkenny et al. (1999).

Velocity data from the two nights were phased to the pulsation cycle using the ephemeris of Kilkenny et al. (1999): $T_0 = 2\,449\,477.4691(\pm0.0016)$, Period $= 0.1065784(\pm0.0000005)$d. The measured radial velocities were multiplied by the factor -1.42 to correct for projection effects and give the surface velocity through the pulsation cycle in the stellar rest frame. The projection factor was chosen based on preliminary work by Montañés Rodriguez et al. (2000) (See also Albrow & Cottrell 1994; Gautschy 1987; and references therein). We will discuss later the effects of choosing a different projection factor. A smooth curve (high order polynomial) was fit to the velocity data (Fig. 2). The velocity values on this curve were used to calculate change in stellar radius ($\Delta R_\star$) and surface acceleration. The phase bin centers for acceleration and $\Delta R_\star$ are shifted by half a bin with respect to the velocity bins, i.e. the end of an acceleration bin is the center of the next velocity bin and the end of a velocity bin is the center of the next $\Delta R_\star$ bin.

3.2. Temperature determination

To find temperature variations through the pulsation cycle, synthetic spectra were fit to the ground-based BV photometry of Kilkenny et al. (1999) and our HST ultraviolet spectrophotometry. Before the fitting, the spectra were binned in wavelength. No information is lost through the binning since the fits are to the shape of the spectrum, not to individual lines. The spectra are noisy at short wavelengths, reflecting a drop in detector sensitivity. To avoid possible problems caused by this increased noise, only the part of the spectra with $\lambda \geq 1270$ Å was used.
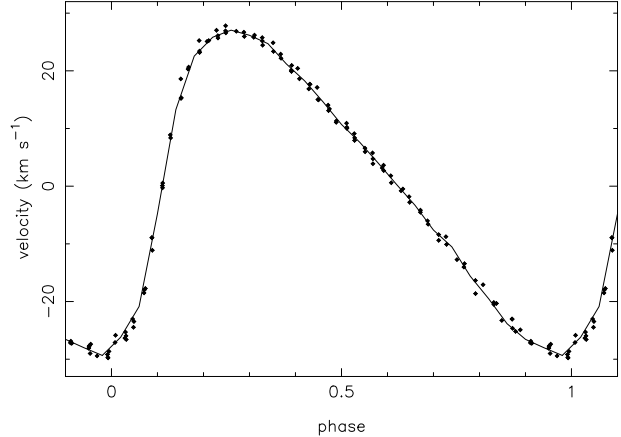

Fig. 2. Fit (solid line) to velocity data corrected for projection effects (points). The data have been folded over by 0.2 cycles in Figs. 2, 4, and 5.

The pulsation period was divided into phase bins and the spectra and photometry within each bin were averaged. No significant difference in the results was found with the period divided into 15, 25, 50, or 99 bins. We will report the results found for 25 bins.

A grid of line-blanketed model atmospheres was calculated under the assumption of plane-parallel geometry, hydrostatic equilibrium and local thermodynamic equilibrium using the code STERNE described by Jeffery & Heber (1992) and by Drilling et al. (1998). Following the latter, we assumed a composition for LSS 3184 given by $n_H = 0, n_{He} = 0.99$ and $n_C = 0.003$, where n represents fractional abundance by number, and all other elements were assumed to have solar-like relative abundances. The grid extended between $15\,000$ and $30\,000$ K, $\log g = 3.00$ and 4.00 (cgs units). As will be shown later, changing the $\log g$ used in the model atmospheres makes only a minor difference in the temperatures and angular radii derived.

In the fitting procedure $T_{\rm eff}$, angular radius (α), and E_{B-V} were allowed to vary and the downhill simplex program AMOEBA (Press et al. 1992) was used to find the minimum χ^2 difference between the synthetic spectrum and the observed spectral and photometric data at each phase (Jeffery et al. 2000). An example of the fit is shown in Fig. 3.

When the extinction E_{B-V} was allowed to vary we found the mean to be $E_{B-V} = 0.239 \pm 0.008$. Because the extinction is not expected to vary with pulsation phase, we chose to use $E_{B-V} = 0.24$ throughout the cycle and did a second iteration allowing only temperature and α to vary.

3.3. Radius determination

In determining the radius of LSS 3184, we make two assumptions. First, we assume that the temperature (and
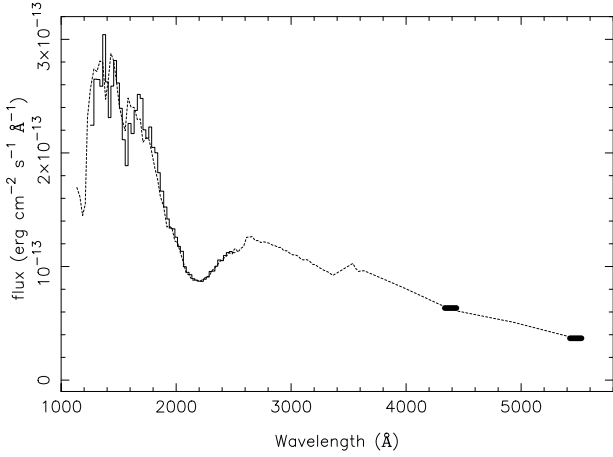
Fig. 3. Best fit synthetic spectrum (dashed curve) plotted with ultraviolet spectrum (histogram) and BV photometry values. This is for the phase bin centered at 0.580.

thus α) and radial velocity (and thus $\Delta R_\star$) were measured at approximately the same layer in the stellar atmosphere. Second, because we measure α perpendicular to the line of sight and $\Delta R_\star$ parallel to the line of sight, we are assuming that the pulsation is spherically symmetric. Thus we get $\Delta R_\star / R_\star = \Delta \alpha / \alpha$. With these assumptions we can use a modified Baade's method (Baade 1926) to find $R_\star$, using our previously determined values of α and $\Delta R_\star$.

There are two ways we can do this. In the first, we choose two phase bins, determine $\Delta \alpha / \alpha$ and $\Delta R_\star$ between them and find $R_\star = \Delta R_\star \alpha / \Delta \alpha$, with α and $R_\star$ defined at one of the chosen phase bins. This method has the disadvantage of using data from only two phase bins and thus ignoring additional information available from the rest of the pulsation cycle. In the second method we plot $\Delta \alpha / \alpha$ versus $\Delta R_\star$. The slope of a linear fit to the data points is then $1/R_\star$. We use the second method.

4. Results and discussion

The velocities, effective temperatures, and angular radii measured through the pulsation cycle of LSS 3184 are listed in Table 1. The velocities are not corrected for projection effects and are reported for the center of the phase bins. Temperatures and angular radii are reported for the beginning of the phase bins. Data are missing where HST observations did not fall in the affected phase bins. Typical uncertainties are indicated.

The surface acceleration, surface velocity, and change in radius determined for LSS 3184 using the AAT spectra are shown in Fig. 4. Note that the surface velocity reported here is the velocity measured from the spectra multiplied by -1.42 to correct for projection effects and make positive velocity be away from the star's center. The change in radius has been set so that it is zero at photometric maximum, $\phi = 0$.

Table 1. Velocity, temperature, and angular radius through the pulsation cycle of LSS 3184. Velocity is not corrected for projection effects.

ϕ bin range	V^a (km s^{-1}) ± 0.40	$T_{\text{eff}}{}^b$ (K) $\pm 90.$	α^b (10^{-11} arcsec) ± 0.005
0.00–0.04	18.58	22500	1.799
0.04–0.08	14.80	22480	1.799
0.08–0.12	3.39	22480	1.794
0.12–0.16	-9.42	22450	1.790
0.16–0.20	-16.00	22350	1.793
0.20–0.24	-18.31	22230	1.796
0.24–0.28	-19.18	22040	1.807
0.28–0.32	-18.56		
0.32–0.36	-17.53	21700	1.831
0.36–0.40	-15.04	21500	1.846
0.40–0.44	-12.94	21340	1.857
0.44–0.48	-10.36	21180	1.867
0.48–0.52	-7.59	21100	1.868
0.52–0.56	-5.38	21000	1.874
0.56–0.60	-2.82	20940	1.877
0.60–0.64	-0.19	20930	1.876
0.64–0.68	2.36	20900	1.877
0.68–0.72	5.39	20900	1.877
0.72–0.76	7.47	20990	1.870
0.76–0.80	11.07	21100	1.864
0.80–0.84	13.85	21330	1.849
0.84–0.88	16.91	21540	1.840
0.88–0.92	18.83	21750	1.832
0.92–0.96	19.86		
0.96–1.00	20.81	22410	1.802

^{a} center of phase bin
^{b} beginning of phase bin

Fig. 5 shows the integrated flux between 1270 and 2508 Å and the temperature and angular radius determined by fitting synthetic spectra to HST UV spectra and ground-based BV photometry through the pulsation cycle.

$\Delta \alpha / \alpha_0$ is plotted against $\Delta R_\star$ in Fig. 6. The '0' subscript indicates that the reference bin is at $\phi = 0$. As is seen in Figures 4 and 5, the shapes of the α and $\Delta R_\star$ curves are not identical, which is the cause of the non-linear, looped shape of the $\Delta \alpha / \alpha$ versus $\Delta R_\star$ curve. If the α and $\Delta R_\star$ curves are normalized and placed on the same plot (Fig. 7), the differences in the curves are more noticeable. Figure 12 from Kilkenny et al. (1999) shows a similar loop on the right hand side of the angular radius versus stellar linear radius plot. Our work cannot be used as an independent confirmation of the non-linear angular versus stellar radius curve, however, as we have used the same BV photometry as Kilkenny et al.

The non-linear shape makes determining the radius more difficult. It raises questions about the assumption made in using Baade's method to find $R_\star$, that $\Delta R_\star$
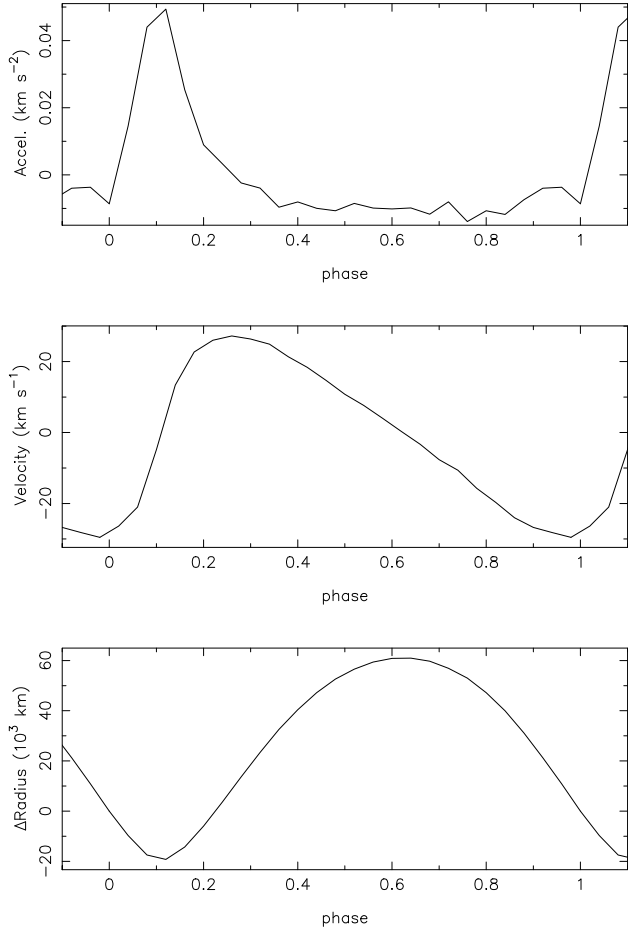
Fig. 4. Surface acceleration, surface velocity, and change in radius of LSS 3184 through its pulsation cycle.

Fig. 5. Flux $\langle F_{1270-2508} \rangle$, effective temperature, and angular radius of LSS 3184 through its pulsation cycle. The curves simply connect the data points and are not fits to the data.

and $\Delta\alpha$ are measurements of the same quantity, with $\Delta\alpha$ decreased by a factor proportional to the distance to LSS 3184. One possible explanation of the discrepancy is that we are measuring $\Delta R_\star$ and α at different layers in the atmosphere. $\Delta R_\star$ is measured using optical spectra, while α is measured using ultraviolet spectra and optical photometry. It is possible that the layer where the optical lines are formed expands and contracts a bit differently than the layer where the ultraviolet continuum is formed. It is also possible that the star and/or its pulsations are not spherically symmetric, as might occur if the star were flattened by rotation, so that the measured $\Delta\alpha$, which is perpendicular to the line of sight, and $\Delta R_\star$, which is parallel to the line of sight, act differently. Further, the atmosphere is not static. The atmosphere's temperature is constantly changing, and the pulsating layers undergo a substantial compression at minimum radius, as shown by the spike in the acceleration in Fig 4, which may cause nonadiabatic effects. So the temperature may be acting differently in the expanding part of the phase than in the contracting part.
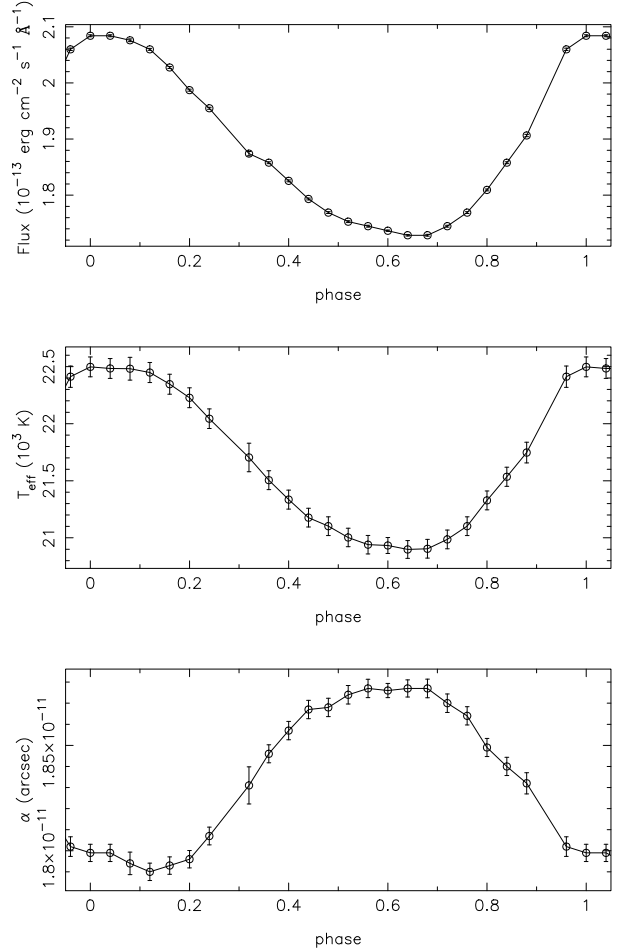
However, it is encouraging that the slopes of the expanding (the upper half of the loop in Fig. 6) and contracting (lower half of the loop) parts of the $\Delta\alpha/\alpha$ versus $\Delta R_\star$ curve are not too different. $\Delta\alpha$ and $\Delta R_\star$ are still correlated.

If we find the slope of the curve using a least squares fit to all of the data points (dashed line in Fig. 6) then the radius at photometric maximum ($\phi = 0$), the inverse of the slope, is $2.27 \pm 0.10 R_\odot$, where the uncertainty is derived from the standard error in the least squares fit to the slope. The average $\Delta R_\star$ over the pulsation cycle, with $\Delta R_\star \equiv 0$ at $\phi = 0$, is $28\,190$ km, or $0.04 R_\odot$. So if we use all the $\Delta\alpha/\alpha_0$ versus $\Delta R_\star$ data points, we find the mean $R_\star$ to be $\langle R_\star \rangle = 2.31 R_\odot$. This is larger than the $1.35 R_\odot$ mean radius found by Kilkenny et al. (1999) for LSS 3184 and is closer to the $1.91 R_\odot$ mean radius found for V652 Her by Lynas-Gray et al. (1984).

We tested the effects of using only a portion of the $\Delta\alpha/\alpha$ versus $\Delta R_\star$ curve to determine $R_\star$, though we have
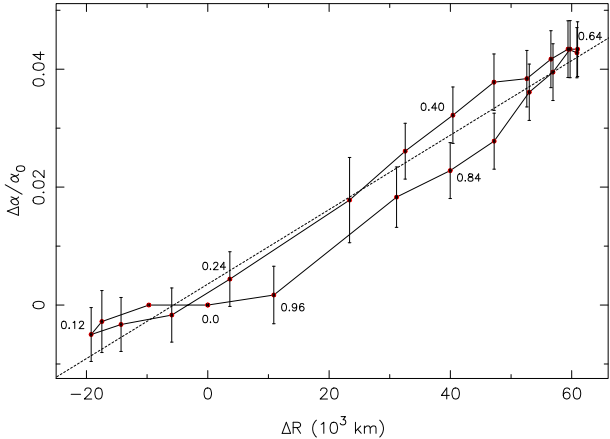
Fig. 6. $\Delta\alpha/\alpha_0$ versus $\Delta R_\star$ through the pulsation cycle of LSS 3184. Points are connected in order of phase with $\phi = 0$ at the origin. The dashed line is a linear least squares fit to all data points. Error bars for $\Delta R_\star$ are smaller than the symbols. Numbers next to symbols indicate the corresponding pulsation phase.
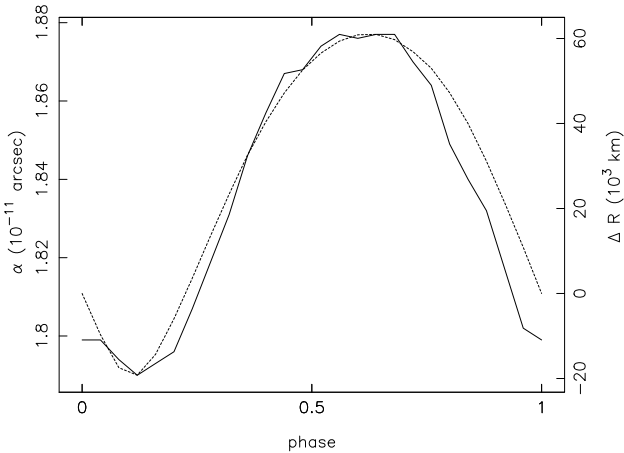

Fig. 7. α (solid curve) and ΔR (dashed curve) versus pulsation phase.

no reason to reject any particular data points. If we use the points on the upper part of the curve, with phase $0.16 \leq \phi \leq 0.56$, then we find $\langle R_\star \rangle = 2.16 \pm 0.07 R_\odot$. If we use the points on the lower part of the curve, ignoring the points to the left of the change in slope at $\Delta R_\star \approx 10\,000$ km, so that $0.60 \leq \phi \leq 0.96$, we find $\langle R_\star \rangle = 1.75 \pm 0.08 R_\odot$. If we use only the points to the right of $\Delta R_\star = 0$ km then we find $\langle R_\star \rangle = 1.97 \pm 0.10 R_\odot$. In all cases, even the extreme one where we reject all points but those on the lower part of the curve, our $\langle R_\star \rangle$ is larger than $R_\star = 1.35 \pm 0.15 R_\odot$, the value found by Kilkenny et al. (1999).

Drilling et al. (1998) estimated $\log g = 3.35 \pm 0.1$ for LSS 3184. If we use this with our $\langle R_\star \rangle = 2.31 R_\odot$ in the formula $g = GMR^{-2}$, we find $M_\star = 0.42 \pm 0.12 M_\odot$.

This is larger than $0.15 M_\odot$, the mass found by Kilkenny et al. (1999) for LSS 3184 and closer to $0.7^{+0.4}_{-0.3}$, the estimated mass of V652 Her (Lynas-Gray et al. 1984). Our larger estimate results mainly from the larger peak-to-peak range of radial velocities we measured. It is likely that the smaller velocity amplitude measured by Kilkenny et al. resulted from a combination of the lower spectral resolution and the lower signal to noise in the spectra they used. This meant that even the best cross correlation template still contained some velocity broadening, thus diluting the velocity amplitude.

There are several sources of uncertainty in our mass determination. Uncertainty in the $\log g$ used is a major contributor. We note that it is impossible to determine the pulsation phase of LSS 3184 when the spectrum used in the analysis of Drilling et al. (1998) was taken in 1985, as $\dot{P}$ is unknown. They estimated the temperature of LSS 3184 at $23\,300 \pm 700$ K. Our data yield a similar value, $\langle T_{\text{eff}} \rangle = 23\,230$ K, if we use $E_{\text{B}-\text{V}} = 0.27$, the extinction they used. However, because temperature, line strengths, and other parameters presumably varied throughout the 1-hour exposure for their spectrum, it is possible that the errors in their temperature and gravity determinations are larger than the formal errors quoted. If we assume that LSS 3184 has the same $\log g$ as V652 Her, $\log g = 3.68$ (Jeffery et al. 1999), instead of $\log g = 3.35$, then we find that it has $M_\star = 0.92 M_\odot$

As mentioned earlier, the model atmospheres used to calculate temperature and angular radius from *HST* UV spectra and ground-based *BV* photometry assumed $\log g = 3.50$. The assumed gravity enters into the stellar parameter calculations in the stellar atmospheres used and in calculating the mass from the radius. Changing $\log g$ in the model atmospheres by 0.50 dex (to 3.00 or 4.00), but using $\log g = 3.35$ to calculate the mass as before, changes the $\langle T_{\text{eff}} \rangle$, $\langle \alpha \rangle$, and $\langle R_\star \rangle$ derived by about 1 per cent, and thus has only a small effect (~ 3 per cent) on the mass derived. The mass finally derived is proportional to g.

Uncertainty in the extinction also adds uncertainty to the stellar parameters calculated. Using $E_{\text{B}-\text{V}} = 0.25$ instead of 0.24 increases the derived $\langle T_{\text{eff}} \rangle$ by 510 K, or about 2 per cent, but changes $\langle \alpha \rangle$ by only 0.2 per cent, and thus has a very minor effect on the derived stellar radius and mass.

The derived radius varies proportionally with the projection factor used to transform the measured stellar radial velocities into surface velocities. For example, using a projection factor of 1.31, as Lynas-Gray et al. (1984) used in their analysis of V652 Her, instead of 1.42 would give $\langle R_\star \rangle = 2.12 R_\odot$ instead of $\langle R_\star \rangle = 2.31 R_\odot$. The smaller radius would give $M_\star = 0.37 M_\odot$ instead of $M_\star = 0.42 M_\odot$.

5. Conclusions

In this paper we report new determinations of the radius ($\langle R_\star \rangle = 2.31 \pm 0.10 R_\odot$) and mass ($M_\star = 0.42 \pm 0.12 M_\odot$) of

the pulsating hydrogen-deficient star LSS 3184. The radial velocity data and temperature measurements are more reliable than those used for previous radius and mass determinations for this star, so our estimates are likely to be closer to the star's actual parameters. Further improvements can be accomplished by improving the $\log g$ and chemical composition estimates for LSS 3184. In addition, there needs to be further study of the difference between the shapes of the angular radius and physical radius curves based on temperature and flux measurements, and radial velocity measurements, respectively. It is important to determine if the difference in shapes is a sign that some of our data or a step in our analysis is flawed, or if there is something happening in the star itself that causes the two measures of radius to behave differently with pulsational phase.

References

Albrow M. D., Cottrell P. L., 1994, MNRAS 267, 548

Baade W., 1926, Astr. Nachr. 228, 359

Drilling J. S., Jeffery C. S., Heber U., 1998, A&A 329, 1019

Gautschy A., 1987, Vistas in Astron. 30, 197

Jeffery C. S., Heber U., 1992, A&A 260, 133

Jeffery C. S., Hill P. W., Heber U., 1999 A&A 346, 491

Jeffery C. S., Starling R. L. C, Hill P. W, Pollacco D., 2000, MNRAS submitted

Kilkenny D., Koen C., 1995, MNRAS 275, 327

Kilkenny D., Koen C., Jeffery C. S., Hill N. C., O'Donoghue D., 1999, MNRAS 310, 1119

Lynas-Gray A. E., Schönberner D., Hill P. W., Heber U., 1984, MNRAS 209, 387

Montañés Rodriguez P., Aznar Cuadrado R., Jeffery C. S., Pollacco D., 2000, in Szabados L., Kurtz D. (eds.), ASP Conf. Ser., The Impact of Large-Scale Surveys on Pulsating Star Research (IAU Coll. 176), in press

Press W. H., Teukolsky S. A., Vetterling W. T., Flannery B. P., 1992, Numerical Recipes in FORTRAN, 2nd edn. Cambridge Univ. Press, Cambridge

Saio H., 1993, MNRAS 260, 465

Saio H., 1994, in Jeffery C. S., ed., CCP7 Newsletter No. 21, Univ. St Andrews, p. 50

Saio H., 1995, MNRAS 277, 1393